Journal of
Ceramic Science
and Technology

J. Ceram. Sci. Tech., 07 [01] 53-64 (2016)
DOI: 10.4416/JCST2015-00024
available online at: http://www.ceramic-science.com

Superhydrophilic Ceramic Glazes for Sanitaryware

F. Knies[1, 2], K. Schrantz[1, 3], C. Aneziris[2], L. Gauckler[4], T. Graule*[1, 2]

[1]EMPA – Swiss Federal Laboratories for Materials Science and Technology,
Laboratory for High Performance Ceramics, Switzerland
[2]TU Bergakademie Freiberg, Institute for Ceramics, Glass and Building Materials, Germany
[3]Department of Inorganic and Analytical Chemistry, University of Szeged, Hungary
[4]ETH – Swiss Federal Institute of Technology, Switzerland

received June 10, 2015; received in revised form August 14, 2015; accepted September 10, 2015

Abstract

Based on industrial $ZrSiO_4$ glazes for sanitaryware, a new glaze with photoactive oxides was developed. The development aimed to produce a glaze that is smooth in order to decrease contamination of the ware and increase superhydrophilic wetting behaviour for easier cleanability. The glazes were characterized with profilometry, atomic force microscopy, x-ray diffraction and scanning electron microscopy. For reactivity under UV light, the wetting angles in the dark and after irradiation, as well as the degradation of methylene blue were measured. Samples with TiO_2 showed no improvement in wetting, neither in the dark, nor under UV irradiation. However, compared with the industrial $ZrSiO_4$ tile, the cleaning properties were improved in the case of bulk contaminants like mustard. Even more promising results were achieved by replacing $ZrSiO_4$ with ZnO. The glazes developed in this work showed surface roughness of less than 20 nm and superhydrophilic wetting under UV illumination.

Keywords: Glaze, superhydrophilicity, photoactivity, UV irradiation, ZnO, TiO_2

I. Introduction

As water becomes more and more precious as a resource on earth, every household must strive to reduce consumption. Industry also needs to support the rising standards with the regard to the use and treatment of water.

Glazes used to be developed not only to improve the appearance of ceramic products, but also to make them more resistant to environmental influences. Glazes exhibit resistance to chemical attack, e.g. by water, acid or bases[1]. In homes, especially in the bathroom, glazes are exposed to strong and ongoing chemical attack by cleaning agents. Although homeowners may use these cleaning agents with a clear conscience, they also pollute the water as it is difficult to separate the cleaning agents from it. Therefore it is not only necessary to reduce water consumption, for example with water-saving shower heads or WC flushing systems, but also to make glazes that can be effectively cleaned with water alone. Self-cleaning surfaces have been of great interest in the past years [2, 3, 4, 5]. So far, they have been used successfully as coatings on windows [6, 7], where they don't experience too much chemical or mechanical attack. Such sol-gel coatings have been adapted to sanitaryware, but here they are exposed to far more chemicals. Consequently, their lifetime cannot compete with the lifetime of the ceramic substrate. This work aims to develop a new ceramic glaze that combines the traditional requirements of durability and appearance with the self-cleaning properties of the coating.

* Corresponding author: thomas.graule@empa.ch

Ceramic glaze, as used for sanitaryware, consists typically of silica for glass forming, fluxes for improvement of melting behaviour and an opacifier for appearance. Commonly used opacifiers are SnO_2, ZrO_2 or $ZrSiO_4$. SnO_2 shows good opacifying behaviour, even in small quantities, but it is relatively expensive [8]. ZrO_2 forms $ZrSiO_4$ during the melting process at high temperatures and is also more expensive than $ZrSiO_4$, which makes $ZrSiO_4$ the most convenient material for opaque glazes [9].

TiO_2 is also reported to be an opacifier. In the form of anatase, it is reported to produce a white glaze [10]. In both its forms, anatase and rutile, it is used because of its photocatalytic activity [11, 12]. Anatase is frequently referred to as being photochemically more active than rutile [13]. Owing to its rather broad bandgap (3.2 eV), UV irradiation is necessary to create oxygen vacancies. The reduced oxygen leads to the decomposition of organic contamination. Water molecules can attach to the oxygen vacancies and form a layer that washes away inorganic contamination [14, 15]. The drawback of using anatase is that it turns into rutile at around 800 °C. As a result, it loses a significant degree of photoactivity. As sanitaryware is fired at 1250 °C, and a second firing step at lower temperatures for an additional glaze is not desired, an appropriate alternative to TiO_2 has to be found. As the bandgap of anatase is considered appropriate for the process, we looked for oxides with similar bandgaps. ZnO, with a bandgap of 3.2 eV, is also described as having photoactive properties [16, 17]. In higher quantities, it is also considered an opacifier [18, 19]. It reduces glaze viscosity and surface tension, which promotes

the spread of the glaze melt over the surface and improves the chemical durability of the glaze [20].

The aim of this work was to develop a single-firing glaze for sanitaryware with a super smooth surface, in order to avoid contamination in the first place, and with superhydrophilic wetting properties, induced by photocatalytically active components, to facilitate the cleaning process.

II. Materials and Methods

To investigate the influence of TiO_2 and ZnO on the properties of the glaze and on the formation of photocatalytic surface properties, the initial amount of 12 % $ZrSiO_4$ in the glaze was partially replaced.

(1) Materials and processing

The glaze is based on an industrially used standard composition made from SiO_2 as the main glass former (58 wt%), intermediate oxides like Al_2O_3 (10 wt%), net modifiers like Na_2O (17 wt%) and $ZrSiO_4$ (12 wt%) as an opacifier. All materials come from mined raw materials like sand or feldspar. The as-prepared glaze suspension was stirred for 1 h to homogenize it. During the homogenization process, the water content was adjusted to 29 wt%. The modified glazes were prepared by weighing the amount of industrial glaze without $ZrSiO_4$ and by adding the desired amount of oxide and $ZrSiO_4$ (Table 1), in the ratio as presented in Table 2. Milling balls (10 mm, Inframat Advanced Materials, USA, yttria-stabilized zirconia) were added depending on the amount of powder in the suspension. The suspension was ball-milled for 1 h. To improve the application process, 2.7 % carboxymethyl cellulose (CMC, Phrikolat Drilling Specialties GmbH, Germany) binder was added to the suspension and stirred until it was completely dissolved. For the application of the glaze suspension, the ceramic substrate, a 10 x 15 cm tile made from green sanitaryware porcelain (approx. 60 % quartz, 20 % kaolin, 20 % feldspar), was wetted with water to reduce the sorption of the glaze into the tile and consequently better thickness control. For each tile, the suspension was poured over the surface until 30 g of suspension was adsorbed. As the surface quality of the poured glaze influences the surface quality of the fired glaze, this step had to be performed carefully, so as not to leave any flow marks. After they had been glazed, the tiles were dried for 1 h at 100 °C. The samples were co-fired in an electric furnace (Carbolite HTF 17/10, United Kingdom) at a heating rate of 2 K/min. After reaching the dwelling temperature of 1250 °C, which was kept for 45 min, the samples were cooled down at a cooling rate of 2 K/min.

Table 1: Materials used in processing.

Oxide	Manufacturer	D_{50} [µm]	Purity [%]
$ZrSiO_4$	Helmut Kreutz GmbH	1.6	> 99
TiO_2 Rutile	Kronos	1.3	> 99
TiO_2 Anatase	Sigma-Aldrich	0.7	> 99
ZnO	Fluka	0.6	> 99
CMC	Phrikolat	-	98.5

The sample names which follow in the discussion include the amount of oxide in % (compared to the amount of $ZrSiO_4$ in the industrial glaze, taken as 100 %) and abbreviations for the used compounds (Z: $ZrSiO_4$, T: TiO_2 rutile, TA: TiO_2 anatase, Zn: ZnO).

In spite of the phase changes that occur in the glaze during the firing of the samples, the initial denotation was kept through the whole manuscript for easier reading and to keep consistency. To avoid confusion, the oxides are referred to as initially incorporated oxides.

(2) Surface roughness

To get a first evaluation of the surface roughness, an Alpha-Step D-120 mechanical profilometer from KLA-Tencor, USA was used. For the measurements, the samples were cleaned with ethanol to remove organic residues and just before the measurement they were spray-cleaned with filtered compressed air to remove dust particles. The roughness was measured over a length of 10 mm. The speed of the tip was 0.2 mm/s with a force of 10 mg, to keep the tip from picking up vibrations caused by surface defects. Data were filtered with the Alpha-Step software to differentiate roughness from waviness of the glaze surface, and mean roughness (R_a) and maximum roughness (R_y) were calculated.

On the basis of the results obtained with the mechanical profilometer, the samples with the lowest roughness were chosen for further measurements with the atomic force microscope (Mobile S, Nanosurf, Switzerland). To avoid coincidence with surface quality owing to inhomogeneous distribution of crystals on the surface, areas of 10 × 10 µm and 50 × 50 µm were measured in contact mode and with a PPP-NCRL-10 tip.

Table 2: Ratio of oxides and $ZrSiO_4$ in the samples.

$ZrSiO_4$ in the glaze [wt%]	12	9.6	7.2	4.8	2.4	0
Amount of $ZrSiO_4$ [%] compared to the added TiO_2 or ZnO	100	80	60	40	20	0
TiO_2 or ZnO in the glaze [wt%]	0	2.4	4.8	7.2	9.6	12
Amount of TiO_2 or ZnO [%] replacing $ZrSiO_4$	0	20	40	60	80	100

(3) Wetting angle

As the glaze surfaces are not perfectly even and homogeneous, but exhibit a certain roughness owing to e.g. crystallization or pinholes, the wetting model of Wenzel [21, 22] was chosen for evaluation. Wenzel's theory postulates that a liquid spreads until it comes to its equilibrium, providing the topology of the surface does not hinder the droplet from spreading. Problems in the Wenzel theory have been reported with regard to the dependence between roughness and droplet size [23]. As the droplet size of a volume of 10 µl (d ≈ 4 mm) is much bigger than the roughness of few microns, it can be assumed that the roughness does not affect the wetting. Therefore the sessile drop method was chosen over the needle-in-drop method. The sessile drop method was also considered the more applicable method to evaluate critical drops staying on the surface.

Wetting angle measurements were performed with the OCA 20 instrument from Dataphysics, Germany. To remove organic surface contamination, samples were cleaned with ethanol and isopropanol just before the measurement. To remove any dust residues, the surface was sprayed with filtered, compressed air. Drops of pure water of a size of 10 µl are applied with the sessile drop method. The dynamics of the droplet on the surface was recorded and analysed with the SCA 20 software from Dataphysics. Ten measurements were performed on each sample. The samples were measured (I) after keeping them in the dark for 12 h and (II) after 4 h of UV illumination. The samples were illuminated in a BIO-LINK® crosslinker chamber (Vilber Lourmat, France) containing 5 × 8W UV lamps (Philips Pro TL Mini, 365 nm). The UV-illuminated samples were again sprayed with filtered air to cool them down and the wetting angle was measured at room temperature (20 °C).

To ensure that the measurements were not influenced by the atmosphere, a second set-up (Contact Angle Measuring System G2, Krüss GmbH, Germany) was used, under the same experimental conditions as described above. The samples were cleaned as described, but kept in water during the UV illumination, to avoid overheating and further contamination from the atmosphere.

(4) Photodegradation of methylene blue

Photocatalytic activity of the glazes was followed based on the degradation of methylene blue (3,7-bis(Dimethylamino)-phenothiazin-5-ium chloride, MB, Acros Organics, purity > 82 %, CAS 61 – 73 – 4) under visible light, with and without UV pre-treatment of the samples. 3 × 3 cm active surface of the glazes was covered with 40 cm^3 1×10^{-5} mol dm^{-3} MB solution. After 90 min adsorption period in the dark, which was experimentally determined to be sufficient to reach the adsorption equilibrium (based on the steady-state concentrations), the samples were irradiated with visible light in a chamber containing 5 × 8 W lamps (Philips Pro TL Mini 8W/840), covered by a UV filter. To remove the IR radiation, a quartz glass vessel filled with water (height 3 cm) was placed over the samples. Samples of the MB solution were taken during 4 h and their UV-VIS spectra were measured with spectrophotometry (Varian, Cary 50 Scan) over the 200 – 750 nm range. The Beer-Lambert law was used to correlate the maximum absorbance at 665 nm to the MB concentration. The presented results are the average of at least three measurements.

(5) Cleaning tests

For the evaluation of the cleaning performance of the tiles, two contaminants were chosen: a mixture of 40 % Fe_2O_3 (Fluka AG, Switzerland, > 99.9 %, d_{50} = 0.53 µm) and 60 % oleic acid (Sigma-Aldrich, Switzerland, 67 %) according to DIN EN ISO 10545 – 14 [24] and mustard (Bautzner, Germany) according to the description of the Labor L+S AG in Germany [25]. Before the contaminants were applied with an injection needle (d = 0.5 mm), the samples were cleaned with ethanol and isopropanol and dried at room temperature. After the contaminants had been added to the sample surface, the samples were attached to a dip coating device (DipMaster-50, Chemgat Technology Inc., USA), to be cleaned in a dipping step with water (400 ml). As an unknown amount of water always adheres to the sample (pores, surface), this method was used only for qualitative evaluation of the cleaning performance. Two different dipping speeds were used: 100 mm/min (slow) and 500 mm/min (fast), both with 100 repetitions.

(6) Surface-analysing methods

To analyse the surface of the samples, x-ray diffraction (XRD) spectroscopy and scanning electron microscopy (SEM) were used. The XRD analysis of the phase formation in the glaze was conducted with Panalytical X'Pert Pro instrument. SEM images were captured based on measurement of back-scattered electrons (BSE mode) and secondary electrons (SE mode), with a Tescan Vega Plus and a Tescan Vega 3 with EDX.

III. Results and Discussion

(1) Surface roughness

The measurements with the profilometer showed an increase in the roughness with decreasing amount of $ZrSiO_4$ and increasing amount of TiO_2 in its two forms, rutile and anatase (Fig. 1). Apart from the medium value, the standard deviation also increased, owing to an increase in surface defects.

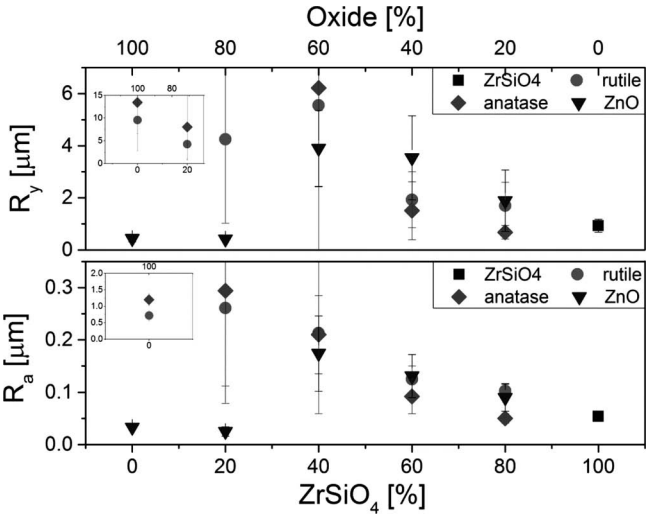

Fig. 1: Surface roughness, measured with profilometer, the $ZrSiO_4$-sample represents the glaze with 12 % $ZrSiO_4$

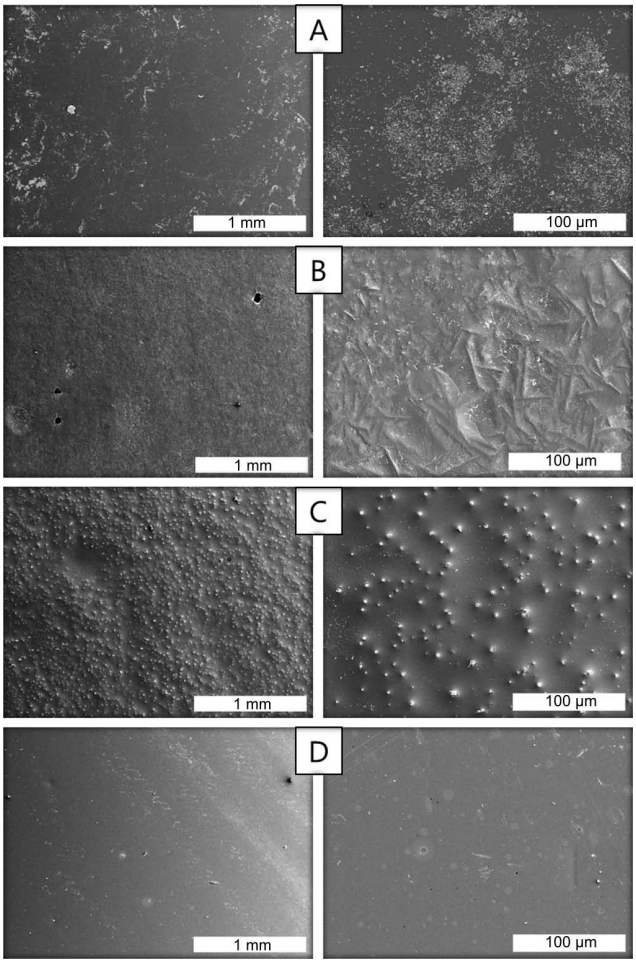

Fig. 2: SEM images of the glaze surfaces containing (A) 12 wt% $ZrSiO_4$ (100Z), (B) 12 wt% rutile (100T), (C) 12 wt% anatase (100TA), (D) 12 wt% ZnO (100Zn); size bar: 1 mm (left column), 100 µm (right column)

Compared to the initial glaze with a roughness of R_a = 55 nm (R_y = 0.95 µm), the replacement of $ZrSiO_4$ with TiO_2 caused an increase of the roughness as a function of the amount replaced. Already a replacement of 20 % of the initial amount of $ZrSiO_4$ led to an increased roughness of R_a = 103 nm (R_y = 0.68 µm) for rutile and a similar roughness R_a = 50 nm (R_y = 0.68 µm) for anatase. While a lower content of anatase influenced the roughness less than rutile, it reached a comparable roughness at an amount of 60 % and 80 %, both with R_a = 210 nm and R_a = 280 nm respectively, which in the graph (Fig. 1) is represented by slightly overlapping symbols. The maximum roughness R_y differed more, which indicates more surface defects, like pinholes, in the glaze containing anatase. A full replacement of $ZrSiO_4$ with TiO_2 led to strong crystallization and therefore a significant increase of the roughness to R_a = 714 nm (R_y = 9.58 µm) for initially rutile-containing glaze and R_a = 1200 nm (R_y = 13.44 µm) for initially anatase-containing glaze (Fig. 1). The SEM images in Fig. 2 A show needle-like crystals measuring about 40 µm in length for the rutile-containing sample and pinch-shaped crystals of 2 to 4 µm in diameter for the anatase-containing sample. The XRD analyses shown in Fig. 3 and Fig. 4 indicate the formation of sphene, a calcium titanium nesosilicate crystal ($CaTiSiO_5$) from rutile and the formation of rutile from anatase [10].

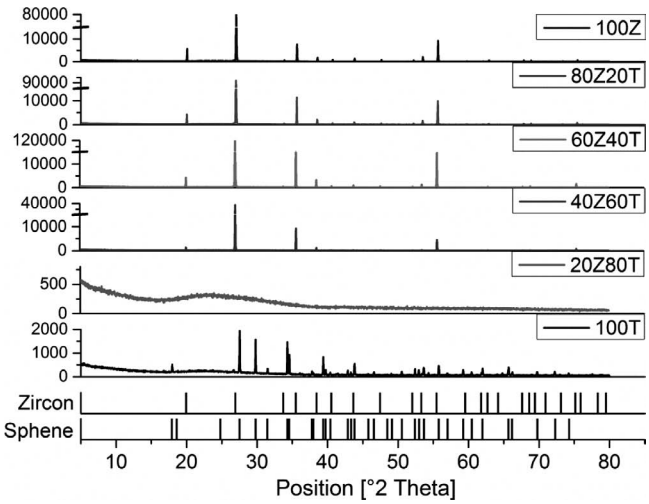

Fig. 3: XRD of samples with rutile; sample names include the amount of oxide (%) compared to total amount of $ZrSiO_4$ and abbreviations (Z: $ZrSiO_4$, T: TiO_2 rutile)

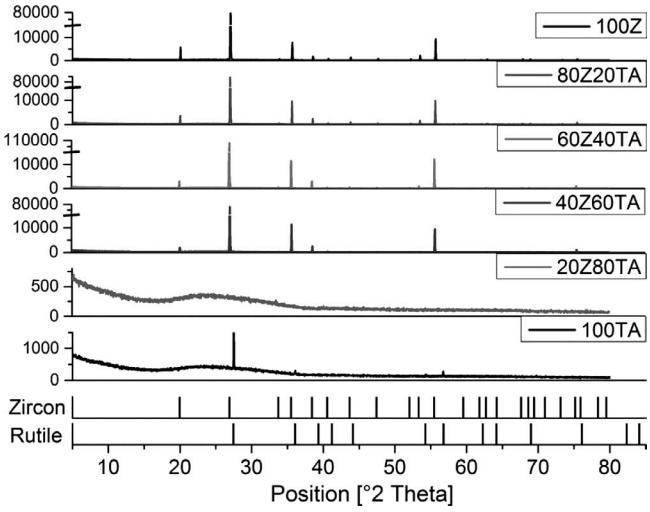

Fig. 4: XRD of samples with anatase; sample names include the amount of oxide (%) compared to total amount of $ZrSiO_4$ and abbreviations (Z: $ZrSiO_4$, TA: TiO_2 anatase)

At a replacement of 80 % initial $ZrSiO_4$ with both anatase and rutile, the glaze became amorphous, respectively the crystalline content was below the XRD detection limit. With further SEM investigation, some crystals could be found around pinholes and also across the surface (Fig. 5 A, B). EDX measurements showed a homogeneous distribution of the elements, which indicates crystal formation from the melt without change in the composition. The roughness could be therefore determined based on the viscosity of the glaze and the melting behaviour. According to Castilone [9], a $ZrSiO_4$ content of less than 3 wt% dissolves in the melt and does not recrystallize in the glaze, so the crystallinity cannot influence the roughness in these samples.

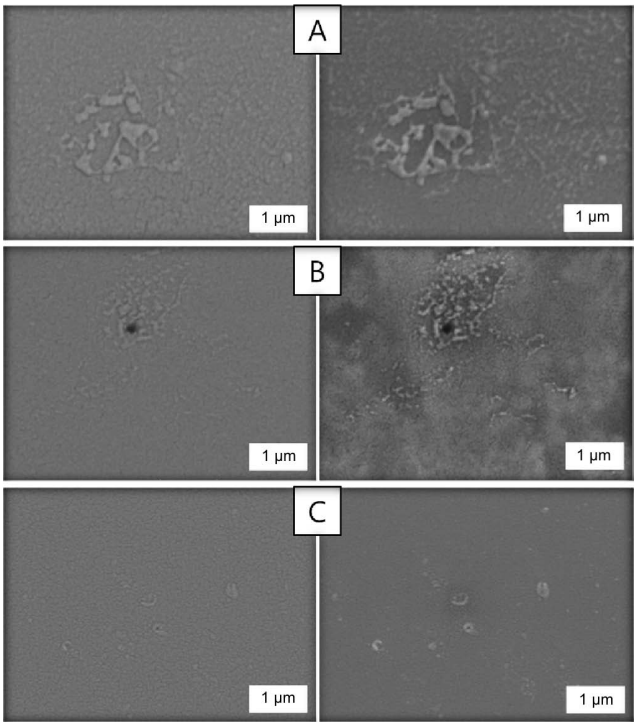

Fig. 5: SEM images of (A) 9.6 wt% rutile (20Z80T), (B) 9.6 wt% anatase (20Z80TA), (C) 12 wt% ZnO (100Zn); BSE mode (left column), SE mode (right column); size bar: 1 µm.

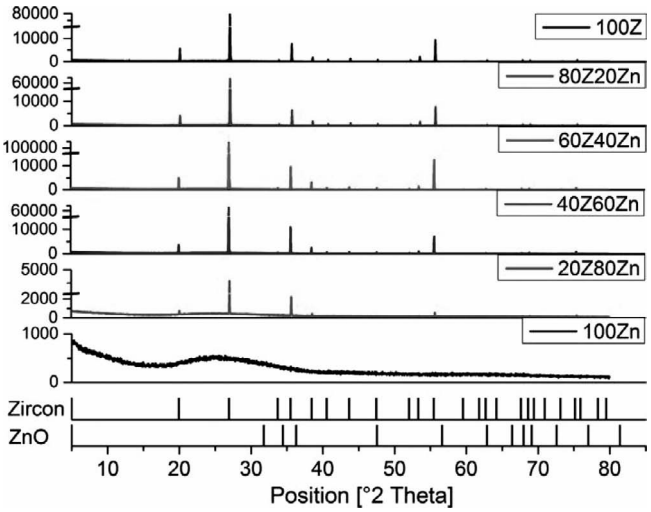

Fig. 6: XRD of samples with ZnO, sample names include the amount of oxide (%) compared to total amount of $ZrSiO_4$ and abbreviations (Z: $ZrSiO_4$, ZnO: Zn).

The XRD diffractogram of samples with higher $ZrSiO_4$ content (above 4.8 wt% in the glaze) shows only the characteristic values of $ZrSiO_4$ crystals at 27°, 34°, 55.5° as presented in Fig. 6. In none of the ZnO-modified samples could ZnO be detected, leading to the conclusion that it had dissolved in the amorphous matrix of the glaze. The added $ZrSiO_4$ content exceeds its solubility limit in the glaze, therefore the excess of $ZrSiO_4$ recrystallizes in proportion to the initially added amount [9]. Therefore the surface roughness should increase with higher $ZrSiO_4$ content and higher crystallinity. Interestingly, in the present samples the opposite behaviour was observed as the concentration of recrystallized particles was high and therefore the crystallites were hindered in their growth. This possibility was supported by SEM images (Fig. 7).

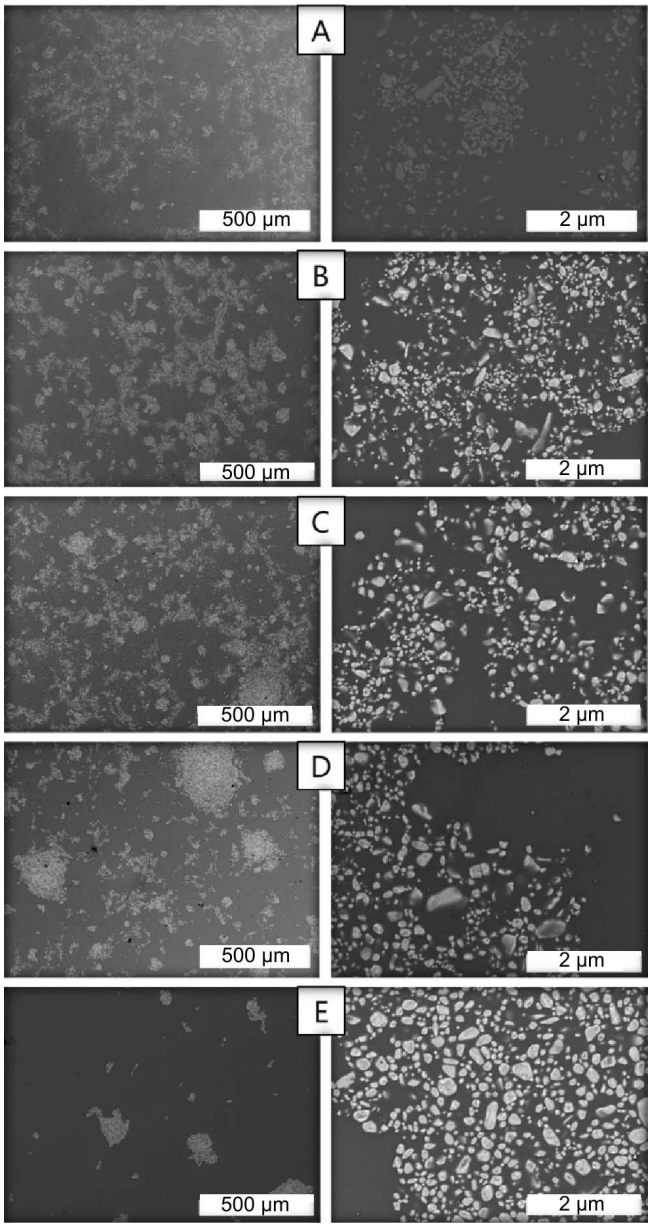

Fig. 7: BSE images of the glazes with ZnO for particle size and distribution (A) 12 wt% $ZrSiO_4$ (100Z), (B) 9.6 wt% $ZrSiO_4$ (80Z20Zn), (C) 7.2 wt% $ZrSiO_4$ (60Z40Zn), (D) 4.8 wt% $ZrSiO_4$ (40Z60Zn), (E) 2.4 wt% $ZrSiO_4$ (20Z80Zn) (Z =$ZrSiO_4$, Zn =ZnO); size bar: 500 µm (left column), 20 µm (right column).

Samples with initial ZnO also showed an increase of the roughness to R_a = 180 nm, up to a ZnO content of 60 %, because ZnO in frits promotes $ZrSiO_4$ precipitation [20]. At a ZnO content of 80 %, the roughness decreased significantly down to R_a = 25 nm. Unlike in the samples with TiO_2 (both anatase and rutile), $ZrSiO_4$ did not dissolve completely, respectively it recrystallized in a higher amount. The amount of ZnO worked more strongly as a flux that smoothed the surface [26] and the recrystallized amount of $ZrSiO_4$ was low, so that the crystals showed less impact on the surface roughness. In a high amount, ZnO is often presented as an opacifier [18, 19]. A full replacement of $ZrSiO_4$ with ZnO and therefore a relatively high amount of 12 % ZnO in the glaze still led to an amorphous and transparent glaze with crystals not traceable by means of XRD (Fig. 6) but with SEM (Fig. 5C). According to Pekkan and Karasu [27], ZnO can be used as an opacifier if the amount of MgO-CaO-ZnO is about 25 mol% and a certain ratio between Al_2O_3 and MgO-CaO-ZnO is achieved, which was not the case in the glaze described here. The high amount of ZnO also reduced pinholes and other surface defects that occurred at lower contents. El-Meliegy *et al.* [19] also mention that ZnO blocks the formation of quartz owing to increasing dissolution of silica during melting, which explains the amorphousness of the glaze.

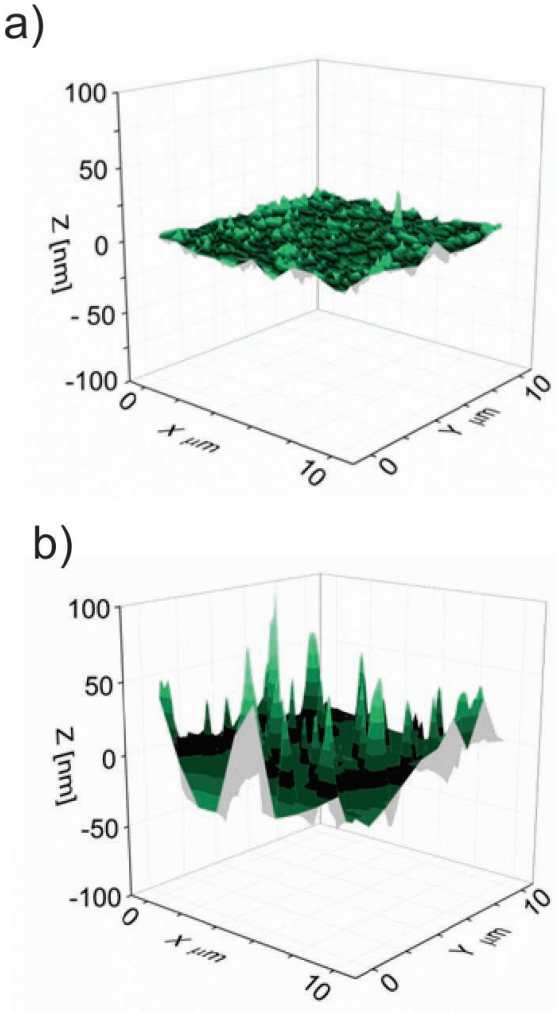

Fig. 8: AFM graph of 12 wt% ZnO glaze (100Zn, a)) and 12 wt% $ZrSiO_4$ (100Z, b)).

In Fig. 7, the BSE images of the ZnO series are presented. The images on the left give an overview of the area, which is covered by crystals. Image calculations showed that the coverage of crystals decreased from 22.5 % for the sample with 12 % $ZrSiO_4$ to a coverage of 2.5 % for the sample 20Z80Zn. The images on the right have higher magnification, allowing better evaluation of the particle size and distribution within the crystal island. With decreasing content of $ZrSiO_4$, the mean particle diameter increases from 0.5 µm to 1.2 µm. The distance between the particles gets smaller. This leads to higher area coverage within the $ZrSiO_4$ crystal islands from 15 % to 33 % with decreasing $ZrSiO_4$ content. This phenomenon is based on the air rising within the glaze owing to degassing of the substrate as described by Wang *et al.* [28]. The increasing particle size explains the increasing roughness with increasing ZnO amount (and decreasing $ZrSiO_4$ amount). With a ZnO content of 9.6 % in the glaze (sample 20Z80Zn), the glassy phase outperformed the crystal phase in the roughness measurement, resulting in a smoother surface.

(2) Wetting angle

The aim of this work was to develop a glaze that changes its wetting behaviour under irradiation. For this purpose, measurements of (I) samples kept in the dark and (II) samples kept under UV irradiation are compared.

(a) *Wetting of samples kept in the dark*

In Fig. 9, the wetting angles of samples kept in the dark are presented. The industrial sample with 12 % $ZrSiO_4$ showed a wetting angle of 36° (±4°) after being kept in the dark. This value was used as a reference value for the modified samples as we aimed to achieve lower wetting angles. Replacing $ZrSiO_4$ with TiO_2, which increased the surface roughness, also increased the wetting angle. When rutile was used as a source of TiO_2, the wetting angles lay between 33° (±4°) and 40° (±3°), but did not show a clear trend in relation to the amount of rutile added. According to selected literature, for some morphologies, surface roughness improves wetting [29, 30, 31], but in this work no correlation could be detected [21]. The addition of anatase to the glaze worsened the wetting slightly more than rutile. With anatase, contact angles of 37° (±2°) to 42° (±5°) were measured. Also here no clear correlation between the wetting angle and the initial amount of anatase, as well as between wetting and roughness of the glaze could be found.

The difference in the wetting angle of samples initially containing anatase and rutile is most probably due to the further transformation of anatase to rutile and of rutile to sphene. Sphene has been shown to be hydrophilic and improve its hydrophilic properties with the increase of the firing temperature [32]. The firing time of the glazes was not long enough for the formation of sphene from rutile, formed in the samples initially containing anatase. Therefore sphene is present only in the initially rutile-containing samples (see XRD in Figs. 3 and 4), resulting in a slightly lower wetting angle in these samples.

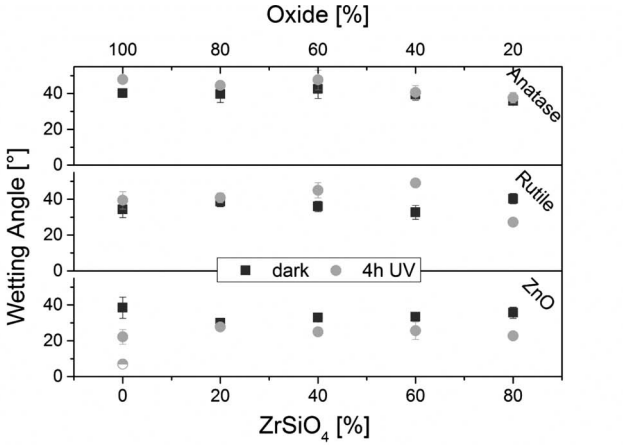

Fig. 9: Wetting angles in the dark and under UV illumination; the half-filled point at 12 wt% ZnO (100Zn) shows the wetting angle after 2 min waiting time after UV illumination.

As in case of 20 % $ZrSiO_4$ replacement with anatase, also a replacement with 20 % of ZnO did not influence the wetting angle, compared to the initial glaze. As ZnO addition promotes the recrystallization of $ZrSiO_4$, the surface roughness increased with the increasing amount of ZnO. The wetting angle on the other hand decreased slightly, as presented in Fig. 9. As the roughness significantly decreased for the sample with 80 % ZnO, the wetting angle in the dark exhibited the lowest value of 30° (±1°). The wetting angle of the sample with a full replacement of $ZrSiO_4$ with ZnO increased again up to 38° (±6°). Even though there are slight changes in the wetting angle, no correlation to glaze composition or surface roughness could be detected. Small changes in wetting angles could be easily induced by changes in the laboratory atmosphere, even when temperature and humidity are kept constant. In the melting process of the glaze, the components show different surface energies of the melt. SiO_2 has the smallest surface energy of 70 – 500 mJ/m² and is therefore likely to cover the other components and determine the wetting angle.

(b) ***Wetting of samples after 4 h UV irradiation***

The wetting angles of the initially rutile-, anatase- and ZnO-containing glazes after 4 h of UV irradiation are presented in Fig. 9. These values were measured on samples illuminated in laboratory atmosphere. To exclude the influence of contamination from air, all measurements were repeated with samples kept under deionized water during illumination [33]. These results confirmed those collected on samples exposed to laboratory atmosphere during UV illumination. The unmodified sample with 12 % $ZrSiO_4$ (sample 100Z) had a wetting angle of 36° (±4°). After UV illumination, this increased slightly to 42° (±4°). The difference between these values is not significant, suggesting no relevant effect of UV irradiation on this sample.

After 4 h of UV irradiation of rutile-containing samples, the one with 20 % rutile showed a decrease in the wetting angle from 40° (±3°) to 28° (±2°). The sample containing 40 % rutile showed the highest change: the wetting angle increased from 33° (±4°) up to 50° (±2°). Glazes with higher amounts of rutile showed a lower increase in the wetting angle, and between 80 % and 100 % rutile, there was no significant change in the wetting angle of irradiated samples in comparison with the samples kept in the dark.

The samples with anatase showed a slight increase in the average wetting angle after UV illumination, but this is not significant compared to the samples kept in the dark.

In the XRD data, neither rutile nor anatase could be detected, owing to the strong $ZrSiO_4$ signal. As rutile forms from anatase at around 800 °C, anatase should be completely transformed in the glaze. As in the sample with 60 % TiO_2 (for both rutile and anatase samples) and 40 % $ZrSiO_4$, the $ZrSiO_4$ can be detected, but no form of TiO_2. It is possible that the TiO_2 dissolved in the glaze or its content was below the detection limit.

Wetting angle measurements after UV illumination of the samples with ZnO as a photoactive oxide showed a sudden decrease in the wetting angle in the whole series. The highest decrease could be achieved with 20 % addition of ZnO and with full replacement of $ZrSiO_4$ by ZnO. ZnO is listed as a photoactive oxide [34] but cannot be detected in the XRD measurements. Therefore it is not clear to what extent the photoactivity, which is more pronounced in a crystalline state of the oxide, influences the wetting. As the amount of ZnO in the glaze is relatively low (2.4 – 12 wt%), it tends to act as a flux and be dissolved in the amorphous matrix.

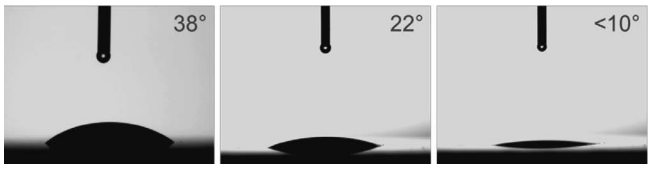

Fig. 10: Wetting angle of glaze with 12 wt% ZnO (100Zn); left: in the dark, middle: after 4 h UV, right: after 4 h UV after 2 min.

For the sample with 12 wt% ZnO, that is a full replacement of $ZrSiO_4$, we were able to detect time-dependent wetting. In the dark, this sample showed a wetting angle of 38° (±6°). After UV illumination, an instant drop down to 22° (±2°) was observed. In the next two minutes, the droplet continued spreading and achieved an angle of less than 10°, which could no longer be accurately measured with the software. The corresponding series of images is presented in Fig. 10. Time dependence of ZnO wettability had already been shown on thin films and surfaces with diverse morphology [35, 36], where the wetting angle decreased under continuous UV illumination. In the measurement presented here, the intense UV illumination was stopped after 4 h, while during the wetting angle measurement the sample was still under the influence of visible light illumination. The time dependence of the wettability as observed within this work cannot be definitively explained at present. According to the current knowledge on this phenomena, the reversible wettability of ZnO could be explained by the competition between the adsorption and desorption of surface hydroxyl groups and the rearrangement of the organic chains (if present) on the surface. However, the kinetics of these processes also depend on the ZnO morphology. It could also be possible that during initial spreading the droplet reaches particles with a morphology that promotes hydrophilicity. This approach

could be supported by the findings of Khranovskyy *et al.* [36], since (based on SEM images, Fig. 5 C), the morphology of the 100Zn sample surface is not homogeneous. However, in case of sample 100Zn it has to be kept in mind that ZnO is present together with SiO_2 (and several other components of the glaze) at the sample surface, which broadens the possible explanations.

(c) ***Photoactivity under visible light***

As discussed previously, both TiO_2 and ZnO are known to be photocatalytically active semiconductors [11 – 17]. Owing to their relatively broad band gap (~ 3.2 eV), they are mainly used under UV light, either in suspensions [37], immobilized [38, 39], or in contact with a gas phase [40]. Nowadays glazes have to fulfil specific needs, like self-cleaning [20, 41], photocatalytic [20, 42], and antibacterial properties [43], therefore it would be favourable to synthesize active surfaces using simple and cheap materials. A few groups report on photocatalytic activity of different glazes under UV light [42, 44], however, for practical application, the production of visible-light-active glazes would be preferable.

To simulate the everyday use of the TiO_2- and ZnO-containing glazes, in this work their photoactivity was followed based on the degradation of MB under visible light. MB is often used as a model compound to monitor the efficiency of the catalyst [45, 46], owing to its good adsorption properties which allow charge transfer between the catalyst and the dye, as well as the possibility to easily follow its degradation with UV-Vis spectroscopy.

Fig. 11 shows chosen degradation curves of MB in contact with the industrial glaze and the one with 40 % ZnO content, after 4 h visible light illumination, compared to the blank. The time needed to reach the adsorption equilibrium at the surface of the samples was determined to be ~ 90 min (see the Experimental section). The concentration of MB measured after this time was considered to be the initial concentration (c_0).

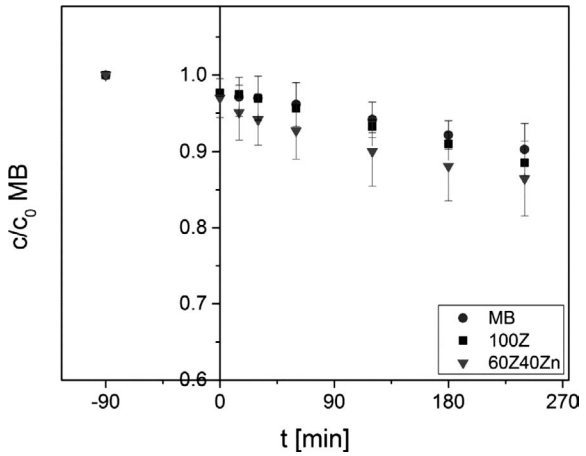

Fig. 11: Degradation of MB in contact with the industrial glaze with 12 wt% $ZrSiO_4$ (100Z) and the glaze with 7.2 wt% $ZrSiO_4$ (60Z40Zn) content during 4 h visible light illumination, compared to the blank (MB).

It can be seen that although there is a small difference in the MB degradation on these two surfaces, it is within the error of the measurement. For all other samples this difference was even smaller. Fig. 12 shows all the measured data after 4 h of visible light illumination, presented in %. Since during the firing process anatase turns into rutile and rutile to sphene, it is not surprising that there is no measurable difference between the photoactivity of initially anatase- and rutile-containing samples fired at 1250 °C. Besides this, the negligible degradation of MB on these samples is most probably due to the complete absence of UV irradiation and the very small content of these compounds in the glaze overall.

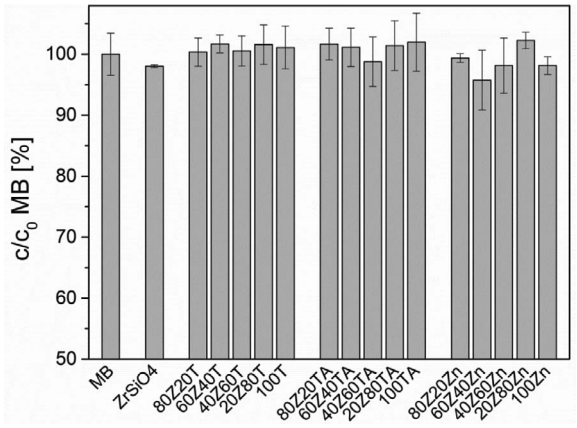

Fig. 12: MB concentration (%) after 4 h visible light illumination, in contact with all the investigated samples, compared with the industrial glaze ($ZrSiO_4$, sample 100Z) and the blank (MB).

Since the wetting angle measurements after UV illumination of samples with ZnO showed a sudden decrease in the wetting angle in the whole series, we also tested the photoactivity of these samples after 4h of UV illumination (Fig. 13).

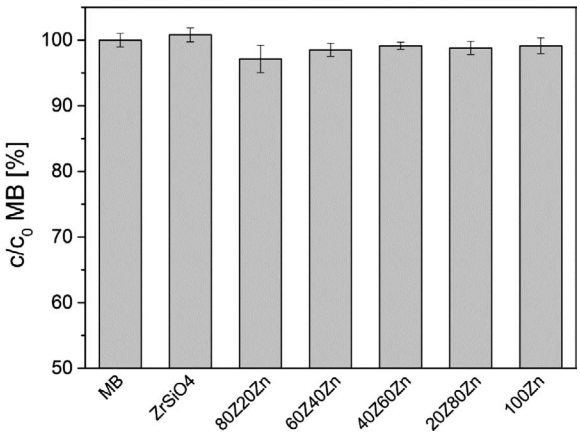

Fig. 13: MB concentration (%) after 4h visible light illumination, in contact with the industrial glaze ($ZrSiO_4$) and ZnO containing samples, pre-treated with 4h of UV illumination.

The highest decrease in the wetting angle was seen for samples with 20 % ZnO content and with full replacement of $ZrSiO_4$ by ZnO. The former sample also showed slightly higher (although still not significant) photoactivity compared to other samples. This, however, could not be observed for the $ZrSiO_4$ industrial glaze. No straightforward correlation between the wetting angle and the photoactivity of the UV pre-treated samples can be claimed. In general, visible light absorption can be enhanced with modification of the semiconductor band gap, e.g. by doping [40], or it can also be tuned by controlling the crystallization process in the glaze [42, 44]. One explanation for the absence of

photoactivity can be the very small amount of ZnO in the glaze and the spreading of amorphous silica over the surface, covering the ZnO crystals. The absence of ZnO XRD signals supports this conclusion. However, amorphous silica contributes to smoothing of the glaze surface, which, on other hand, favours the small wetting angle.

(c) ***Cleaning tests***

For the cleaning experiments, contaminants (Fe_2O_3-oleic acid-mixture and mustard) were homogeneously applied to the cleaned glaze surface. Then the contaminated samples were cleaned in a dipping process, as shown in Fig. 14.

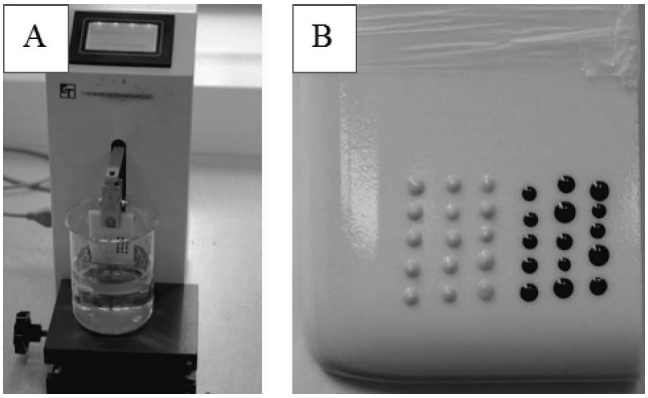

Fig. 14: (A) Set-up cleaning tests and (B) contaminated sample; mustard (white dots), Fe_2O_3-oleic acid-mixture (dark dots).

The results showed a clear dependence of the cleanability on the roughness. Samples with a roughness higher than R_a = 200 nm (initially 12 % rutile (100T), 12 % anatase (100TA), 9.6 % rutile (20Z80T), 9.6 % anatase (20Z80TA)) had a significantly decreased cleanability in the case of the Fe_2O_3-oleic acid-mixture as the contaminant, compared to the industrial glaze with 12 wt% $ZrSiO_4$. It seems that the contaminant deposits in the surface structure and the water then spreads over it. Especially for the samples with only anatase (100TA) and rutile (100T), it can be seen that the large crystals keep the contaminants sticking at the surface, as shown on selected samples in Fig. 15. This was not the case for smoother tiles initially containing smaller amounts of anatase (40Z60TA, 60Z40TA, 80Z20TA) and rutile (40Z60T, 60Z40T, 80Z20T), as they offer a smaller surface area for the contaminants to adhere to. These samples showed better cleanability compared to the industrial glaze. Interestingly, within the test series containing ZnO, glazes with higher ZnO content (100Zn, 20Z80Zn), having very low roughness, showed lower cleanability than the samples with lower ZnO content, indicating that ZnO seems to increase the oleophilicity of the surface. Samples with lower ZnO content (40Z60Zn, 60Z40Zn and 80Z20Zn) but similar roughness like the corresponding anatase- and rutile-containing samples also showed better cleanability compared to the industrial glaze. Compared to the industrial sample 100Z, all samples with ZnO showed improved cleanability, independent of changes in roughness.

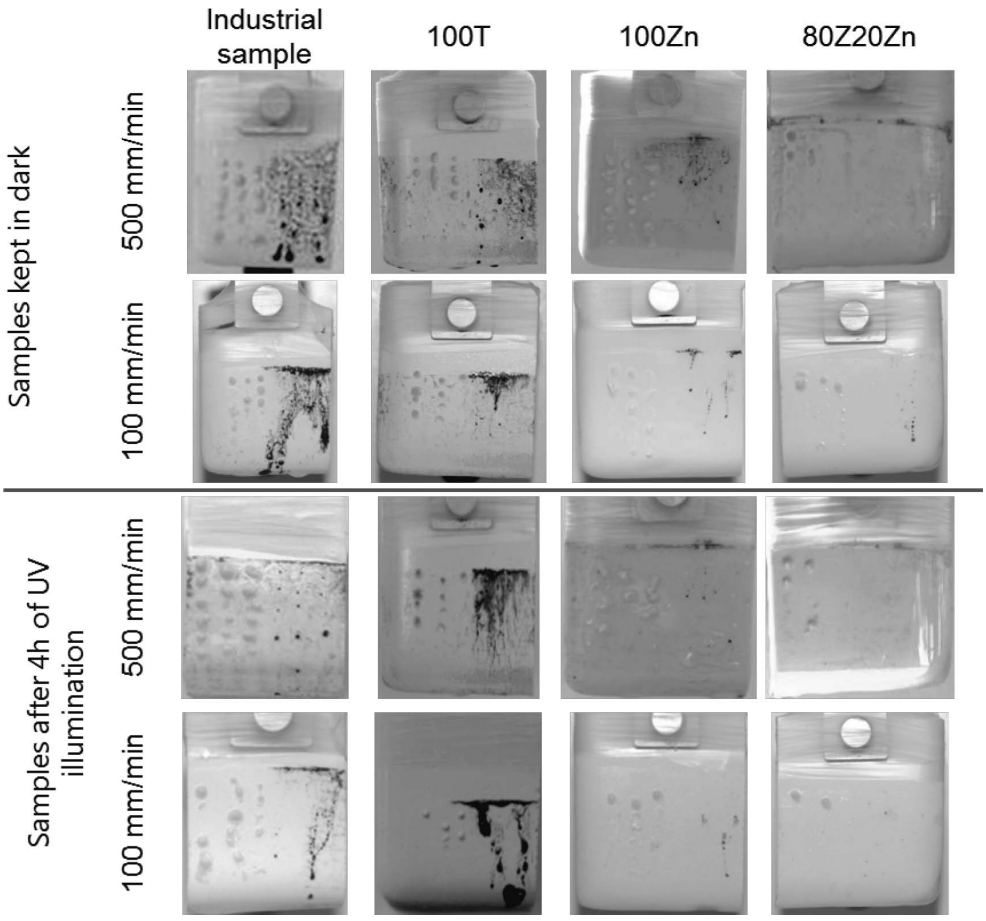

Fig. 15: Samples after the cleaning tests.

In case of the mustard, the industrial glaze showed relatively low cleanability. A significant difference between the industrial sample with 12 % $ZrSiO_4$ (100Z) content and the sample with addition of 2.4 % ZnO (80Z20Zn) was observed, in favour of the latter. With the increasing ZnO content, the cleanability decreased. With full replacement of $ZrSiO_4$ (100Zn), no difference could be seen in the cleaning performance compared to the industrial glaze. TiO_2-containing samples showed much better cleanability compared with both samples with high ZnO content and the industrial glaze.

As mustard could only be applied in bulk and not as a thin layer like the oleic acid-Fe_2O_3 mixture, it is assumed that the mustard does not fully cover the glaze surface, but builds bridges on the peaks of rough surfaces similar to hydrophobic surfaces. The water can then spread between the lower valleys and therefore attack the contaminant from underneath. The oleic acid wets the valleys more and is therefore more difficult to wash away. Therefore, it proved easier to clean the mustard off the rougher samples (100TA, 20Z80TA, 100T, 20Z80T) than it was to remove the Fe_2O_3-oleic-acid-mixture. This is not the case with glazes containing ZnO. The best cleaning results with mustard were shown by the relatively smooth sample, containing 20 % ZnO (80Z20Zn). This indicates that the cleanability does not necessarily change linearly with the roughness; there could be an optimal roughness to achieve the best cleaning behaviour.

The cleaning experiments were also conducted on samples that had been illuminated with UV light for 4 h. The results of selected samples are presented in Fig. 15. An improvement in cleanability with UV illumination could not be achieved on the rough samples (100TA, 20Z80TA, 100T, 20Z80T). As the smoother samples already showed very high cleanability, it was not possible to observe any significant change in the cleanability after the UV irradiation. For the easy-clean samples, a more sensitive test or a more adhesive contaminant has to be found.

IV. Conclusions

In this work, we investigated the effect of the photoactive oxides TiO_2 and ZnO on the roughness, wetting and cleaning behaviour, as well as the photoactivity under visible light of industrial $ZrSiO_4$-opacified glazes. The aim was to develop a smooth surface, preferably with visible light photoactivity, to minimize contamination and maximize superhydrophilicity, in order to improve the cleaning properties of the glazes during every day use.

Samples with TiO_2 showed a strong increase in roughness and no improvement in wetting, neither under dark conditions, nor under UV irradiation. As the photoactive anatase completely transforms into rutile at high temperatures, the absence of significant photoactivity, especially under visible light illumination is understandable. Compared with those of the industrial $ZrSiO_4$ tile, the cleaning properties were improved with bulk contaminants like mustard, but worsened with low-viscosity contaminants like the Fe_2O_3-oleic acid-mixture as a result of the surface topology.

ZnO, as the other choice of photocatalytic active oxide, showed strong improvement in wetting behaviour, even with samples kept in the dark. Under UV irradiation, samples with ZnO showed an immediate hydrophilic behaviour which changed into superhydrophilic wetting behaviour after a droplet age of 2 min. The superhydrophilic behaviour could not be correlated with photoactivity, as the measured decomposition of MB was not significant to allow clear conclusions. The surface roughness changed through a maximum with the addition of ZnO, and decreased significantly with high ZnO amounts. The samples containing ZnO also showed the best cleaning behaviour with the Fe_2O_3-oleic acid-mixture and, with low amount of ZnO, also with mustard. The cleanability is correlated to the roughness, as samples with ZnO showed low surface roughness as well as improved cleanability compared to the rougher samples with TiO_2. The comparison between samples with ZnO did not show a direct correlation with the roughness, but for cleaning of bulk and liquid contaminants, optimal roughness is desired.

Based on the results detailed above, ZnO is a promising additive for glazes and has to be further examined. To enable its use for industrial purposes it also has to be further examined in the context of environmental impact.

Acknowledgement

We appreciate the availability of the Scanning Probe Microscopy User Lab at Empa for the AFM measurement. The authors gratefully acknowledge the financial support from CTI-project no. 14552.2 PFNM-NM.

References

1 Taylor, J.R., Bull, A.C., Ceramics, I. o.: *Ceramics Glaze Technology*, Institute of Ceramics by Pergamon Press, (1986).

2 de Niederhäusern, S., Bondi, M., Bondioli, F.: Self-cleaning and antibacteric ceramic tile surface, *Int. J. Appl. Ceram. Tec.*, **10**, 949 – 956, (2013).

3 Midtdal, K., Jelle, B.P.: Self-cleaning glazing products: A state-of-the-art review and future research pathways, *Sol. Energ. Mat. Sol. C.*, **109**, 126 – 141, (2013).

4 Parkin, I.P., Palgrave, R.G.: Self-cleaning coatings, *J. Mater. Chem.*, **15**, 1689 – 1695, doi:10.1039/B412803F (2005).

5 Piispanen, M., Määtta, J., Areva, S., Sjöberg, A.M., Hupa, M., Hupa, L.: Chemical resistance and cleaning properties of coated glazed surfaces, *J. Eur. Ceram. Soc.*, **29**, 1855 – 1860, (2009).

6 Mills, A., Lepre, A., Elliott, N., Bhopal, S., Parkin, I., O'Neill, S.A.: Characterisation of the photocatalyst Pilkington Activ™: a reference film photocatalyst? *J. Photoch, Photobio. A*, **160**, 213 – 224, (2003).

7 Permpoon, S., Fallet, M., Berthomé, G., Baroux, B., Joud, J.C., Langlet, M.: Photo-induced hydrophilicity of TiO_2 films deposited on stainless steel via sol-gel technique, *J. Sol-Gel Sci. Technol.*, **35**, 127 – 136, (2005).

8 Atkinson, I., Teoreanu, I., Zaharescu, M.: Correlation among composition properties of SnO_2 opacified glazes, *UPB Sci. Bull., Series B*, **70**, 11 – 22, (2008).

9 Castilone, R.J., Sriram, D., Carty, W.M., Snyder, R.L.: Crystallization of zircon in stoneware glazes, *J. Am. Ceram. Soc.*, **82**, 2819 – 2824, (1999).

10 Teixeira, S., Bernardin, A.M.: Development of TiO_2 white glazes for ceramic tiles, *Dyes Pigments*, **80**, 292 – 296, (2009).

11 Linsebigler, A.L., Lu, G., Yates, J.T.: Photocatalysis on TiO_2 surfaces: principles, mechanisms, and selected results, *Chem. Rev.*, **95**, 735 – 758, (1995).

[12] D'Arienzo, M., Siedl, N., Sternig, A., Scotti, R., Morazzoni, F., Bernardi, J., Diwald, O.: Solar light and dopant-induced recombination Effects: photoactive nitrogen in TiO_2 as a case study, *J. Phys. Chem. C*, **114**, 18067 – 18072, (2010).

[13] Sclafani, A., Herrmann, J.M.: Comparison of the photoelectronic and photocatalytic activities of various anatase and rutile forms of titania in pure liquid organic phases and in aqueous solutions, *J. Phys. Chem.,* **100**, 13655 – 13661, (1996).

[14] Fujishima, A., Rao, T.N., Tryk, D.A.: Titanium dioxide photocatalysis, *J. Photoch. Photobio. C*, **1**, 1 – 21, (2000).

[15] Wang, R., Hashimoto, K., Fujishima, A., Chikuni, M., Kojima, E., Kitamura, A., Shimohigoshi, M., Watanabe, T.: Light-induced amphiphilic surfaces, *Nature*, **388**, 431 – 432, (1997).

[16] Rekha, K., Nirmala, M., Nair, M.G., Anukaliani, A.: Structural, optical, photocatalytic and antibacterial activity of zinc oxide and manganese doped zinc oxide nanoparticles, *Physica B.*, **405**, 3180 – 3185, (2010).

[17] Zhou, X., Guo, X., Ding, W. Chen, Y.: Superhydrophobic or superhydrophilic surfaces regulated by micro-nano structured ZnO powders, *Appl. Surf. Sci.,* **255**, 3371 – 3374, (2008).

[18] Bobkova, N.M., Boloban, L.V., Gailevich, S.A.: Phase formation in titanium glazes, *Glass Ceram.*, **54**, 17 – 19, (1997).

[19] El-Meliegy, E., van Noort, R.: *Glasses and glass ceramics for medical applications*, Springer, 2012.

[20] Casasola, R., Rincón, J.M., Romero, M.: Glass-ceramic glazes for ceramic tiles: A review, *J. Mater. Sci.*, **47**, 553 – 582.

[21] Wenzel, R.N.: Resistance of solid surfaces to wetting by water, *Ind. Eng. Chem.*, **28**, 988 – 994, (1936).

[22] Wenzel, R.N.: Surface roughness and contact angle, *J. Phys. Colloid Chem.*, **53**, 1466 – 1467, (1949).

[23] Wolansky, G., Marmur, A: Apparent contact angles on rough surfaces: the wenzel equation revisited, *Colloid. Surface A*, **156**, 381 – 388 (1999).

[24] DIN EN ISO 10545 – 14 (1997).

[25] Schwarzkopf, A. (Labor L+S AG, Germany, 27.11.2013).

[26] Rhodes, D., Hopper, R.: Clay and Glazes for The Potter, 252 (1957).

[27] Pekkan, K., Karasu, B.: Zircon-free frits suitable for single fast-firing opaque wall tile glazes and their industrial productions, *J. Eur. Ceram. Soc.*, **29**, 1571 – 1578, (2009).

[28] Wang, S., Peng, C., Huang, Z., Zhou, J., Lü, M., Wu, J.: Clustering of zircon in raw glaze and its influence on optical properties of opaque glaze, *J. Eur. Ceram. Soc.*, **34**, 541 – 547, (2014).

[29] Borgs, C., De Coninck, J., Kotecký, R., Zinque, M.: Does the roughness of the substrate enhance wetting? *Phys. Rev. Lett.*, **74**, 2292 – 2294, (1995).

[30] Yu, J., Zhao, X., Zhao, Q., Wang, G.: Preparation and characterization of super-hydrophilic porous TiO_2 coating films, *Mater. Chem. Phys.*, **68**, 253 – 259, (2001).

[31] Yu, J., Zhao, X.: Effect of surface microstructure on the superhydrophilic property of the sol-gel derived porous TiO_2 thin films, *J. Mater. Sci. Lett.*, **20**, 671 – 673, (2001).

[32] Cheng, S., Wei, D., Zhou, Y.: Mechanical and corrosion resistance of hydrophilic sphene/titania composite coatings on titanium and deposition and release of cefazolin sodium/chitosan films, *Appl. Surf. Sci.*, **257**, 2657 – 2664, (2011).

[33] Zubkov, T., Stahl, D., Thompson, T., Panayotov, P., Diwald, O., Yates, J.*:* Ultraviolet light-induced hydrophilicity effect on TiO_2(110)(1 x 1). Dominant role of the photooxidation of adsorbed hydrocarbons causing wetting by water droplets, *J. Phys. Chem. B*, **109**, 15454 – 15462, (2005).

[34] Nair, M.G., Nirmala, M., Rekha, K., Anukaliani, A.: Structural, optical, photo catalytic and antibacterial activity of ZnO and co doped ZnO nanoparticles, *Mater. Lett.*, **65**, 1797 – 1800, (2011).

[35] Sun, R.-D., Nakajima, A., Fujishima, A., Watanabe, T., Hashimoto, K.: Photoinduced surface wettability conversion of ZnO and TiO_2 thin films, *J. Phys. Chem. B*, **105**, 1984 – 1990, (2001).

[36] Khranovskyy, V., Ekblad, T., Yakimova, R., Hultman, L.: Surface morphology effects on the light-controlled wettability of ZnO nanostructures. *Appl. Surf. Sci.*, **258**, 8146 – 8152, (2012).

[37] Veréb, G., Ambrus, Z., Pap, Zs., Kmetyko, A., Dombi, A., Danciu, V., Cheesman, A., Mogyrosi, K.: Comparative study on UV and visible light sensitive bare and doped titanium dioxide photocatalysts for the decomposition of environmental pollutants in water, *Appl. Catal. A-Gen.,* **417 – 418**, 26 – 36, (2012).

[38] Kete, M., Pavlica, E., Fresno, F., Bratina, G., Stangar, U.L.: Highly active photocatalytic coatings prepared by a low-temperature method, *Environ. Sci. Pollut. Res. Int.*, **21**, 11238 – 11249, (2014).

[39] Veréb, G., Ambrus, Z., Pap, Zs., Mogyrosi, K., Dombi, A., Hernadi, K.: Immobilization of crystallized photocatalysts on ceramic paper by titanium(IV) ethoxide and photocatalytic decomposition of phenol, *Reac. Kinet. Mech. Cat.*, **113**, 293 – 303, (2014).

[40] Michalow, K.A., Otal, E., Burnat, D., Fortunato, G., Emerich, H., Ferri, D., Heel, A., Graule, T.: Flame-made visible light active TiO_2:Cr photocatalysts: correlation between structural, optical and photocatalytic properties, *Catal. Today*, **209**, 47 – 53, (2013).

[41] Zhang, J., Severtson, S.J.: Fabrication and use of artificial superhydrophilic surfaces, *J. Adhes. Sci. Technol.*, **28**, 751 – 768, (2012).

[42] Meseguer, S., Galindo, F., Sorli, S., Cargori, C., Tena, M.A., Monros, G.: Vidriados cerámicos con actividad fotoquímica: Aplicación potencial a depuración ambiental. *Ceram. Inf.,* **333**, 61 – 67, (2006).

[43] Yoshida, H., Abe, H., Taguri, T., Ohashi, F., Fujino, S., Kajiwara, T.: Antimicrobial effect of porcelain glaze with silver-clay antimicrobial agent, *J. Ceram. Soc. Jpn.*, **118**, 571 – 574, (2010).

[44] Ruiz, O., Sanmiguel, F., Gargori, C., Galindo, F., Monros, G. in *Proceedings of X World Congress on Ceramic Tile Quality*, 15 – 31.

[45] Senthilraja, A., Subash, B., Krishnakumar, B., Rajamanickam, D., Swaminathan, M., Shanthi, M.*:* Synthesis, characterization and catalytic activity of co-doped Ag-Au-ZnO for MB dye degradation under UV-A light, *Mat. Sci. Semico. Proc.,* **22**, 83 – 91, (2014).

[46] Houas, A., Lachheb, H., Ksibi, M., Elaloui, E., Guillard, C., Herrmann, J.-M.: Photocatalytic degradation pathway of methylene blue in water, *Appl. Catal. B-Environ.*, **31**, 145 – 157, (2001).